The impact of process, thermal variations and materials on waveguides losses

Xinxin Huang

1. Introduction

In the last century, micro electromechanical systems (MEMS) have developed rapidly due to their advantages of small size, light weight, low power consumption and low cost[1]. Such development has brought an increasing interest in the surface characterization of micro devices as it optimizes the device performance. Optical waveguide using silicon-on-insulator (SOI) substrates has generated significant interest, since this technology can be CMOS compatible and offers a wide range of possibilities. The SOI technology bases on the use of a layered silicon-insulator-silicon substrate in place of conventional silicon substrate during the manufacturing of semiconductors. The SOI technology can diminish the parasitic device capacitance and improve performance. There are two major benefits of SOI technology compared to conventional silicon technology. One is the lower parasitic capacitance because of the isolation from the bulk silicon, which increases power consumption at matched performance. The other is resistance to latch up due to complete isolation of the n- and p-well structure[1].

SOI increases chip functionality and does not require the cost of most process equipment changes (such as higher resolution lithography tools). Advanced circuits, basing on multiple layers of SOI-type device silicon, can lead the way to a coupling of electrical and optical signal processing into a single chip. This results in a dramatic broadening of communication bandwidth with new applications such as global ranging, direct-link entertainment and communication to hand-held devices[2].

In the 20th century, several papers discussed the performance of high-index-contrast micro photonic devices based on SOI technology. However, these devices are always limited by the scattering losses caused by the sidewall roughness. If we want to use SOI waveguides for optical communication, both polarization insensitivity and single-mode propagation have to be satisfied at the same time [4]. In order to reach these conditions, we need deeply etched rib SOI waveguides with dimensions of the order of 1 mm. Because of the etching process realized by reactive ion etching (RIE), these devices generally suffer from side-wall roughness [5]. Sidewall roughness is a significant issue for optical devices. Surface roughness has critical effects on the performance and reliability of a micro device [3]. There are two main factors that influence the performance of semiconductor devices [4]. One is intrinsic material losses(e.g. free carrier absorption) and the other is scattering loss from imperfections(e.g. fabrication errors). Waveguide side-wall roughness affects performance because the modes propagating in the waveguide penetrate into the waveguide side-walls, which results in significant scattering losses. Here we are going to discuss the latter situation. We will discuss the 2D analysis and 3D analysis separately.

2. 2D analyses of geometry on scattering losses in planar dielectric waveguides

Many studies have tried to model the effects of roughness and waveguide dimension on scattering losses by 2D models. The most commonly accepted one is the Payne-Lacey(PL) analysis model[5]. Here we want to calculate the scattering losses from a random imperfection of the wall of a slab waveguide, in which the optical power is being transmitted[5]. It uses a closed form expression to describe the scattering losses in 2D ways. The equation is expressed as a function of fundamental waveguide parameters, the root-mean-square(r.m.s) roughness(σ) and the correlation length(L_c).

Mathematical description of roughness

The geometry of strip waveguides looks like Fig.1(reprint from [6]) below. Our goal is to study the effects of sidewall roughness by developing a cover with intentional roughness added to smooth waveguides etch stripes. The silicon core layer is surrounded by a silica cladding. We can also tell the roughness model from Fig.1 (reprint from [6]). From the figure we can tell the top and the bottom of the waveguide are polished. Furthermore, we also assume that the top and the bottom of this waveguide are perfectly smooth, which means there is no roughness on the surface. Since for this kind of model there is only roughness on the left and right side of the waveguide(for stripe waveguide), a 1D figure is enough to display the roughness of the waveguide we are going to calculate. Here we use f(z) to shows the excursions of the real edge. We can think f(z) as the local deviation of the perturbed surface from the perfect smooth waveguide. We always use the autocorrelation to describe the nature of roughness. Usually, it can be approximated as below[5]:

$$R(u) = \langle f(z)f(z+u)\rangle \approx \sigma^2 \exp\left(-|u|/L_c\right) \qquad (1)$$

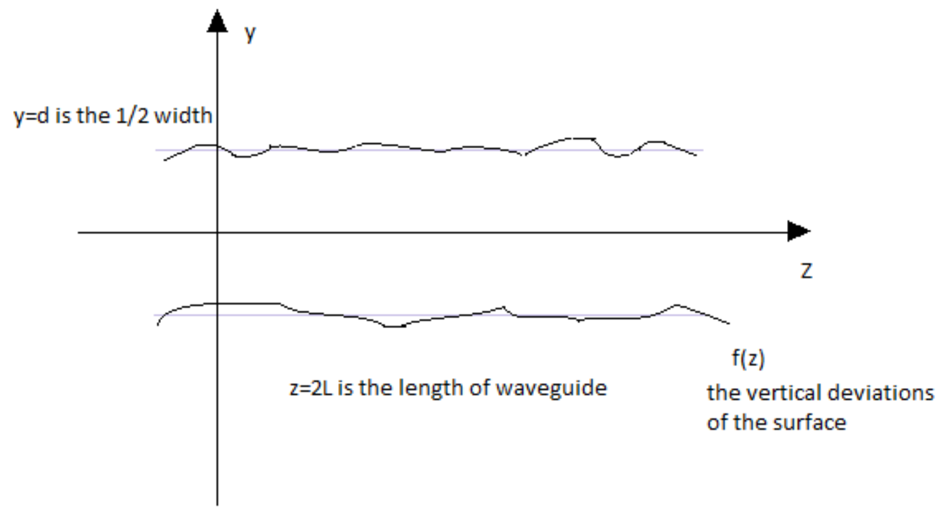

Figure 1 Symmetrical slab waveguide geometry

Here, $<\cdot>$ shows the ensemble average, σ is the standard variance of side wall roughness, and L_c is the correlation length and u is the distant between the side wall roughness surface and the perfect smooth waveguide surface.

In order to calculate the scattering losses, we have to assume a random variance of waveguide width first. As a result, the local variances of effective index are related to a pseudo-grating along the side wall. As a fraction of the dipole cannot be recovered, the scattering loss effect occurs.

It is easy to show that the exponential radiation loss coefficient is [6]:

$$\alpha_r = \frac{P_{rad}/2L}{P_g}$$

Where $P_{rad}/2L$ is the total power radiated per unit length of waveguide, given by

$$\frac{P_{rad}}{2L} = \frac{n_{cl}}{2}\sqrt{(\frac{\varepsilon_0}{\mu_0})\int_0^{\pi}\frac{<|E_x(r,\theta)|^2>}{2L}rd\theta}$$

Where μ_0 is vacuum permeability$\mu_0 = 4\pi * 10^{-7}$, ε_0 is vacuum permittivity$\varepsilon_0 = 8.85 * 10^{-12}$, L is the length of waveguide, ncl is the effective index of waveguide cladding and Ex is the incident electric field. Here we use the polar coordinate to describe the electric field. r is the intensity of the electric field and incidence angle of the electric field.

And P_g is the total guided power, given by

$$P_g = \frac{n_c}{2}\sqrt{\frac{\varepsilon_0}{u_0}\int_{-\infty}^{\infty}\Phi^2(y)dy}$$

nc is the effective index of waveguide core. μ_0 is vacuum permeability and ε_0 is vacuum permittivity we said in the last paragraph. y is the width of waveguide in the Figure1. Thusα_r , the radiation loss coefficient, is given by

$$\alpha_r = \frac{\Phi^2(y)(n_c - n_{cl})^2 {k_0}^3}{4\pi n_c} \int_0^{\pi}\tilde{R}(\beta - n_{cl}k_0 cos\theta)d\theta \ (2)$$

$\Phi(y)$ is normalized so that

$$\int_{-\infty}^{\infty}\Phi^2(y)dy = 1$$

Where Φ^2(y) is a model function depending only on the waveguide geometrical parameter and $k_0 = \frac{2\pi}{\lambda}$ is the wavevector in vacuum. λ is the wavelength of incident wave and θ is the angle of incident wave. $\beta = \frac{2\pi}{\lambda}n_{eff}$ is the propagation constant, neff is the effective index of waveguide. nc is the effective index of waveguide core and ncl is the effective index of waveguide cladding. $\tilde{R}$ is the power spectrum function. Using Wiener-Khintchine theorem [7] to calculate the total radiated power, $\tilde{R}(\Omega)$ is related to the R(u) we got above. The theorem states that the autocorrelation function of a wide-sense-stationary random process has a spectral decomposition given by the power spectrum of that process. For example, if x is a wide-sense stationary process, then we can get the below equation according to the theorem.

$$r_{xx}(T) = \int_{-\infty}^{\infty} e^{2\pi i T f}\, dF(f)$$

Where $r_{xx}(T)$ is the autocorrelation function of the x(t) at every lag T. t represents the time and f is the frequency of the signal. As the theorem, there must be a monotone signal function F(f) that equals to the equation below.

$$r_{xx}(T) = E[x(t)x^*(t-T)]$$

The result shows the total radiated power is the integral of the power carried by each randomly radiate wave. As said by Wiener-Khintchine theorem and Fourier Transformer, we have

$$\tilde{R}(\Omega) = 1/2\pi \int_{-\infty}^{+\infty} R(u) \exp(i\Omega u) du \qquad (3)$$

The autocorrelation function considers the local variances of effective index linked to the evolution side-wall roughness. Furthermore, it reflects the average correlation between one location along the waveguide with another set at distance u [8].

A lot of experimental research has shown that an exponential statistic is well suited to characterize sidewall roughness of larger waveguides [9]. However, as I known, no experimental evidence has been yet reported for submicron type waveguide. As a result, base on equation (1), a sidewall roughness described by an exponential autocorrelation function is assumed in the following such as we can get the scattering loss coefficient in dB/cm [10]

$$\alpha_{cm/dB} = \frac{4.34\sigma^2}{(k_0\sqrt{2}d^4 n_c) g(V) f(x,\gamma)} \quad (4)$$

Where $k_0 = \frac{2\pi}{\lambda}$ is the wavevector in the vacuum, σ is the standard deviation, d is the half width of the waveguide, n_c is the effective index of the waveguide core, g(V) is a function depending only on the waveguide geometry and $f(x,\gamma)$ is linked to the side-wall roughness.

$$g(V) = (U^2 + V^2)/(1 + W) \quad (5)$$

The normalized coefficients are

$$U = k_0 d\sqrt{{n_c}^2 - {n_{eff}}^2} \qquad (6)$$

$$V = k_0 d\sqrt{{n_c}^2 - {n_{cl}}^2} \quad (7)$$

$$W = k_0 d\sqrt{{n_{eff}}^2 - {n_{cl}}^2} \qquad (8)$$

And

$$f(x, \gamma) = \frac{x\sqrt{1 - x^2 + \sqrt{(1 + x^2)^2 + 2x^2\gamma^2}}}{\sqrt{(1 + x^2)^2 + 2x^2\gamma^2}} \qquad (9)$$

Here the x, γ, Δ are

$$x = \frac{W L_c}{d} \qquad (10)$$

$$\gamma = \frac{n_{cl} V}{n_c W \sqrt{\Delta}} \qquad (11)$$

$$\Delta = ({n_c}^2 - {n_{cl}}^2)/(2{n_c}^2) \qquad (12)$$

Using the above equations we plot the figure below. Here nc=3.44, ncl=1.44, lambda is 1.56 um and σ = 6nm, Lc =50 nm.

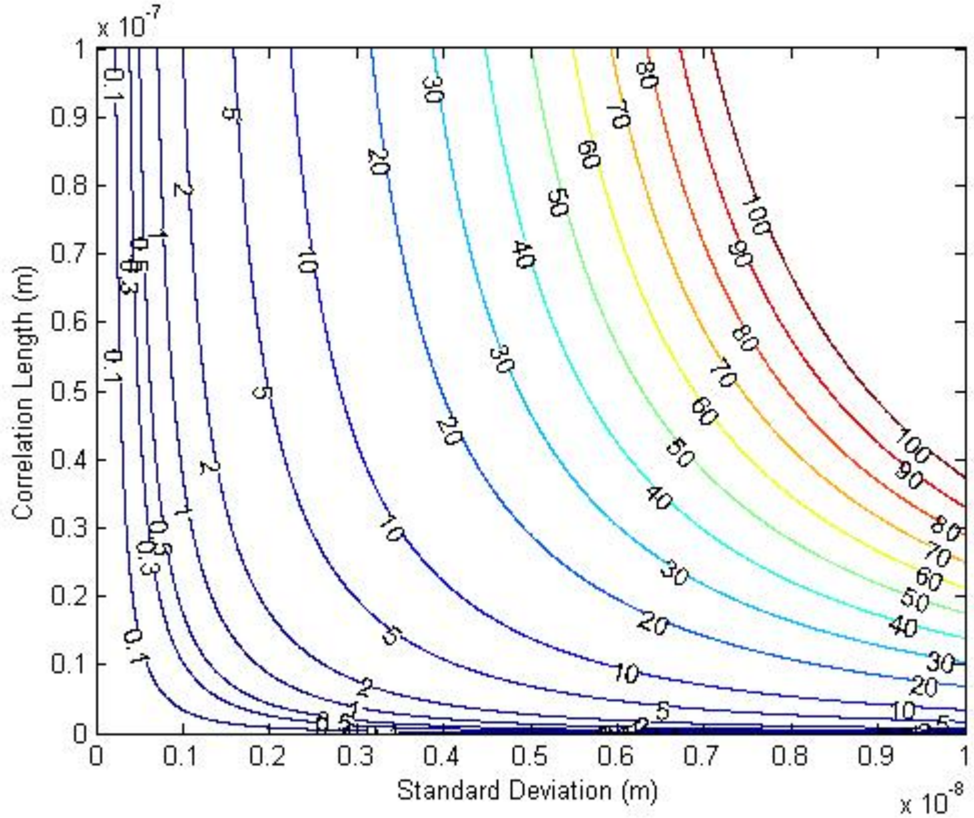

Figure 2 Contour lines of the propagation loss (waveguide width 150nm)

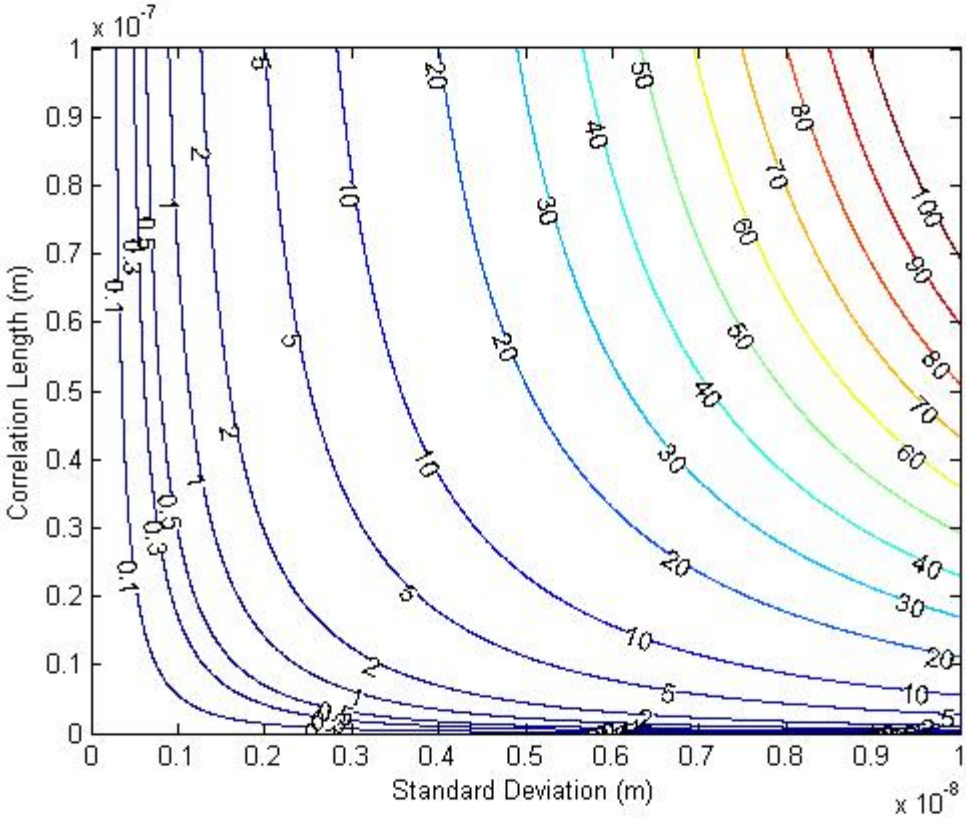

Figure 3 Contour lines of the propagation loss(waveguide width 500nm)

Numerical simulation result shows that the scattering losses of SOI waveguide increases drastically with decreasing of waveguide width. Since the narrower a waveguide is, the stronger interaction of the guided modes with waveguide mode. Also the expression predicts that the scattering loss increase when the surface roughness increase too. And for a given surface roughness, the scattering loss rises as the waveguide dimensions are decreased.

3. 3D analysis of scattering losses due to sidewall roughness in microphotonics waveguide

As we know, there are many reports worked on 2D analysis of scattering losses which limit the performance of micro photonics devices. A popular way to do 2D analysis is to use the effective-index method. The 2D way we discussed in the 2D analysis section was based on this method. Haus indicated that applying a 2D analysis to a strip waveguide assumes an incorrect profile because it does not consider the waveguide of actual rectangle waveguide. The biggest shortage of 2D analysis is that it cannot predict how the cross session affects the transmission performance.

In order to move on, many scientists start to do some 3D work. As we know, it is complicated to use 3D analysis to calculate the scattering losses. Here, the paper [6] presents a leading-order 3D analysis of scattering losses due to sidewall roughness, valid for any refractive-index contrast and field polarization. For the situation of low refractive index contrast waveguide, we would choose to use a simplified 3D method. Then, we could apply the model to all range refractive index contrast situations based on the simple model we built just now.

We need to define all constants: permeability, permittivity, (for both, i.e. free space and waveguide material used), wave number, incident electric field, etc. We define each variable with its known value to be used in calculations. Here, wavelength is defined by λ, wave number by *ki*, permeability of free space by *meu* and permittivity of free space by *eps*, etc. Also, we need to consider the coordinates of incident electric field, to the waveguide and also at the point of observation. The two are discriminated by *x, y, z* and x_c, y_c and z_c. The propagation constant is defined as β. Material parameters are defined as n_{core} and n_{clad}.

Roughness Model

For the convenience of our calculation, we consider the top and bottom walls to be perfectly smooth and let the two sidewalls to have the same roughness statistics. The two roughness statistics are unrelated to each other[7]. This assumption holds in most cases as the top and bottom roughness mostly comes from the deposition process and the sidewall roughness comes from the patterning process[10]. It is only in select polycrystalline materials that the top or bottom roughness may be partially correlated to the sidewall roughness. When uncorrelated, the top and bottom roughness can be considered by adding the scattering losses due to the top and bottom walls to the scattering losses due to sidewall roughness. In summary, the present analysis can be used to get scattering losses.

Initially define the roughness model of the inner sidewalls of waveguide. It is one dimensional vector $f(z)$ with zero mean. Nature of the roughness is described by the autocorrelation function given by:

$$\vec{R}(u) = \langle f(z) f(z+u) \rangle \qquad (13)$$

Here u represents the distant of sidewall roughness from perfect waveguide, z is the length of waveguide. As we get from 2D part we knew that

$$\mathrm{R(u)} \approx \sigma^2 \exp\left(-\frac{|u|}{L_c}\right) \qquad (14)$$

Lc is the correlation length. And use Fourier transform we can get that

$$\tilde{R}(\xi) \approx \int_{-\infty}^{+\infty} R(u) \exp(i\xi u) du \qquad (15)$$

Then by using exponential model, we get the spectral density of roughness

$$\tilde{R}(\xi) \approx \frac{2\sigma^2 L_c}{1 + {L_c}^2 \xi^2} \qquad (16)$$

$\vec{R}(\mu)$ gives the roughness model matrix. This roughness model is being used for calculating the scattering losses in late equation. Where σ is the standard deviation, Lc is the correlation length.

Volume current method (VCM)

The analysis is based on volume current method (VCM) to get the scattering losses. The method is applicable to spheres having small refractive-index perturbation. In this method the internal and scattering fields are approximated with a separation-value solution. And the VCM make all kind of the dielectric constant as equivalent polarization current densities.

Using volume current method, calculated current density vector *J(r)*. Following equations illustrate the calculation involved in calculating *J(r)*.

$$\vec{J}(\vec{r}) = -iw\big(\varepsilon(\vec{r}) - \varepsilon_I(\vec{r})\big)\vec{E} = -iw\delta_\varepsilon(\vec{r})\vec{E} \qquad (17)$$

Here, $\vec{E}$ is the incident electric field, ε is permeability of material of waveguide and free space, and w is the frequency of incident field, waves are input to the function *J(r)*.

Then we can infer the magnetic vector potential $\vec{A}$

$$\vec{A} = \frac{\mathrm{u}}{4\pi}\left(\frac{e^{in_{cl}k_0 r}}{r}\right)\iiint \vec{J}\,(\overrightarrow{r'}e^{-in_1k_0\widehat{\hat{r}r'}})dV' \qquad (18)$$

Where ncl is the refractive index of waveguide, $k_0 = \frac{2\pi}{\lambda}$ is the wavevector in the vacuum, u is the permeability of corresponding waveguide.

The far field pointing vector reduce to

$$\vec{S} = \hat{r}\,\frac{\omega n_1 k_0}{2u}|\hat{r}\times\vec{A}|^2 \qquad (19)$$

Where r is the vector of incident wave, $k_0 = \frac{2\pi}{\lambda}$ is the wavevector in the vacuum, u is the permeability of corresponding waveguide. As a result, the total radiated power is

$$\mathrm{P} = \oiint \vec{S}\cdot\hat{r}dA \qquad (20)$$

Depending on this basic idea, we can then calculate the value of scattering losses. A more exactly electric field can be get from the corresponding dyadic Green's function.

3D analysis model

Base on the roughness model we built before, since the roughness is small compared with the waveguide, we can employ a mode of perfectly waveguide to do the approximation for the waveguide core [12]. This mode can be express as

$$\overrightarrow{E_g(\vec{r})} = \vec{\Phi}(x, y)e^{i\beta z}$$

β is the propagation constant. Then we could replace the waveguide by the following polarization current density

$$\overrightarrow{J_{core}(\vec{r})} = -i\omega\varepsilon_0(n^2(\vec{r}) - {n_{clad}}^2)\overrightarrow{E_g(\vec{r})}(22)$$

Where n_{clad} is the cladding refractive index, $\overrightarrow{n(r)}$ is the refractive-index profile of the rough waveguide, ε_0 is the free-space permittivity.

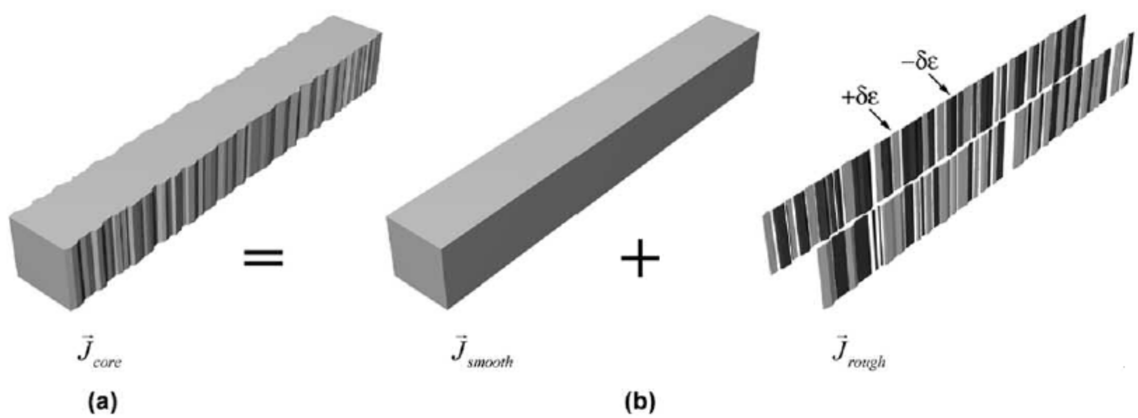

Figure4(reprint from [6]) Decomposition of roughness problem

In order to make the calculation simpler, we decompose the roughness waveguide into two parts. Just removed the perfect part from the waveguide and left the roughness one which need to be calculated alone. As the Figure5(reprint from [6])illustrated. And the current distribution of roughness is express as equation (17).

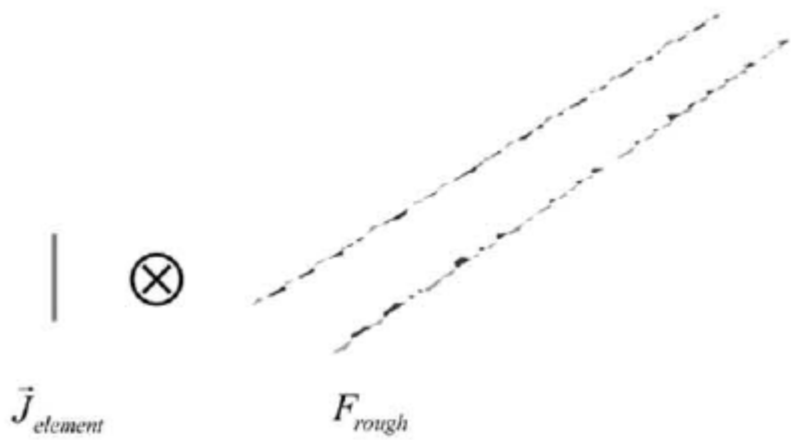

Figure 5(reprint from [6]) A simpler illustration of roughness model

To calculate the far field of J(r), we need to use the array factor here. An array factor is to divide the far field array into several elements of that array. As the Fig.6 (reprint from [6])demonstrated, we use rods of the height of the waveguide to show the roughness. Then the far field of roughness could be found by the below equation:

$$\overrightarrow{E_{rough}} = \overrightarrow{E_{element}} F_{rough} \qquad (22)$$

Where E_{rough} is the far field of roughness, $E_{element}$ is a single rod of the far field. F is the roughness array factor.

Next step is to calculate dyadic green's function[6]. Beside constants like: wave number, points of incident and observation, thickness of the layers etc, we need to calculate: Fresnel reflection coefficient for transverse electric mode *RTE*, Fresnel reflection coefficient for transverse magnetic mode *RTM*, Fresnel transmission coefficient for transverse electric mode *TTE* and Fresnel transmission coefficient for transverse magnetic mode *TTM*.

$$R_{ij}^{TE} = \frac{\mu_j k_{iz_c} - \mu_i k_{jz_c}}{\mu_j k_{iz_c} + \mu_i k_{jz_c}} \quad (23) \qquad\qquad R_{ij}^{TM} = \frac{\varepsilon_j k_{iz_c} - \varepsilon_i k_{jz_c}}{\varepsilon_j k_{iz_c} + \varepsilon_i k_{jz_c}} (24)$$

$$T_{ij}^{TE} = \frac{2\mu_j k_{iz_c}}{\mu_j k_{iz_c} + \mu_i k_{jz_c}} \quad (25) \qquad T_{ij}^{TM} = \frac{2\varepsilon_j k_{iz_c}}{\varepsilon_j k_{iz_c} + \varepsilon_i k_{jz_c}} (26)$$

Here , k is the corresponding wavenumber in different layer of waveguide, u is the permeability of corresponding layer in waveguide, ε_j is the permittivity in j layer of waveguide.

After calculating dyadic green function, it is time to calculate scattering losses in electric field at point of observation whose vector is defined as *r_c*. Form surface current density *Jr* and calculation of dyadic green function *X*, *Erc* is calculated, which is given by following equation;

$$\vec{E}(\vec{r_c}) = iw\mu \iiint \bar{\bar{G}}(\vec{r_c}, \vec{r_c'}).\vec{J}(\vec{r_c})dV'$$

This will results in electric field intensity vector. Then *x, y* and *z* components of electric field intensity vector *Erc* are calculated.

Dyadic Green Function

Now what we need to do is to calculate the green function, from the book[4] we got:

$$\bar{\bar{G}}\left(\vec{r_c}, \overrightarrow{r_c'}\right) = \frac{\frac{i}{8\pi^2} \iint_{-\infty}^{\infty} \left[\bar{\bar{M}}\left(\overrightarrow{k_s}, \vec{r_c}, \overrightarrow{r_c'}\right) + \bar{\bar{N}}\left(\overrightarrow{k_s}, \vec{r_c}, \overrightarrow{r_c'}\right)\right] dk_x dk_y}{k_{mz}|\overrightarrow{k_s}|\text{^}2}$$

Where

$$\bar{\bar{M}}\left(\overrightarrow{k_s}, \vec{r_c}, \overrightarrow{r_c'}\right) = (\overrightarrow{k_s} \times \hat{z_c})(\overrightarrow{k_s} \times \hat{z_c}) e^{i\overrightarrow{k_s}(\overrightarrow{r_s} - \overrightarrow{r_s'})} F_{\mp}{}^{TE}(z_c, z_c{}')$$

And

$$\bar{\bar{N}}\left(\overrightarrow{k_s}, \vec{r_c}, \overrightarrow{r_c'}\right) = \left(\frac{\overrightarrow{k_n} \times \overrightarrow{k_s} \times \hat{z_c}}{i\omega\varepsilon_n}\right)\left(\frac{\overrightarrow{k_m} \times \overrightarrow{k_s} \times \hat{z_c}}{-i\omega\mu_m}\right) e^{i\overrightarrow{k_s}(\overrightarrow{r_s} - \overrightarrow{r_s'})} F_{\mp}{}^{TM}(z_c, z_c{}')$$

Where

$$\vec{k_s} = k_{x_c}\hat{x_c} + k_{y_c}\hat{y_c}$$

Here k_{x_c}, k_{y_c} are the wavenumber in x direction and y direction.

$$F_+(z_c, z'_c) = [e^{ik_{nz_c}z_c} + e^{-ik_{nz_c}(z_c+2d_{n-1})}\widehat{R_{n,n-1}}] \cdot e^{ik_{nz_c}d_n}\widehat{T_{mn}}e^{-ik_{mz_c}d_{m-1}} \cdot [e^{-ik_{mz_c}z_{c'}} + e^{ik_{mz_c}(z_{c'}+2d_{n-1})}\widehat{R_{n,n-1}}]\widetilde{M_m}\widetilde{M'_{n+}}$$

$$F_-(z_c, z'_c) = [e^{-ik_{nz_c}z_c} + e^{ik_{nz_c}(z_c+2d_{n-1})}\widehat{R_{n,n+1}}] \cdot e^{-ik_{nz_c}d_{n-1}}\widehat{T_{mn}}e^{ik_{mz_c}d_{m-1}} \cdot [e^{ik_{mz_c}z_{c'}} + e^{-ik_{mz_c}(z_{c'}+2d_{m-1})}\widehat{R_{m,m-1}}]\widetilde{M_m}\widetilde{M'_{n-}}$$

With

$$\widehat{R}_{i,i+1} = \frac{R_{i,i+1} + \widehat{R}_{i+1,i+2}e^{2ik_{i+1,zc}(d_{i+1}-d_i)}}{1 + R_{i,i+1}\widehat{R}_{i+1,i+2}e^{2ik_{i+1,zc}(d_{i+1}-d_i)}}$$

$$\widehat{R}_{ij} = -\widehat{R}_{ji}$$

$$\widehat{T}_{ij} = \prod_{s=i}^{j-1} \frac{T_{s,s+1}e^{ik_{s,zc}(d_s-d_{s-1})}}{1 - R_{s+1,s}\widehat{R}_{s+1,s+2}e^{2ik_{s+1,zc}(d_{s+1}-d_s)}}$$

Here we can get T and R from equation (23)(24)(25)(26). And di means the width of waveguide i layer, kzc represent the waveguide number in z direction.

Once we calculate the green function then we can have the electric field quickly. Using the components of electric field intensity vector, far field point vector components *Sx, Sy* and *Sz* are then being calculated using the far field Poynting vector:

$$\vec{S}(\vec{r}_c) = \frac{1}{2}Re\left\{\vec{E}(\vec{r}_c)\times\left(\frac{\vec{k}_1}{w\mu}\hat{r}\times\vec{E}^*(\vec{r}_c)\right)\right\}$$

And E is the electric field of incident wave. Re{} means we just take the real number part of he result. w is the frequency of the incident wave and u is the permeability of waveguide. The far field of a point source at the origin is

$$\overrightarrow{E_{pol}}(\overrightarrow{r_c}) = i\omega\mu\bar{\bar{G}}(\overrightarrow{r_c}, \vec{0}) \cdot \overrightarrow{J_{pol}}$$

And also

$$\overrightarrow{J_{pol,y}} = \overrightarrow{J_{pol,z_c}} = -i\omega\epsilon_0({n_{core}}^2 - {n_{clad}}^2)v\widehat{z_c},$$

$$\overrightarrow{J_{pol,z}} = \overrightarrow{J_{pol,-y_c}} = -i\omega\epsilon_0({n_{core}}^2 - {n_{clad}}^2)v\widehat{y_c}$$

In this model, only the two main field components of the first TE and TM-like modes are considered. For calculating far field pointing vectors for rough waveguide for transverse electric mode *SrTE* and for transverse magnetic mode *SrTM*, we need to calculate power array factors for different model, *Fcos* and *Fsin*. For this we need to evaluate:

$$|F_{cos}|^2 = \frac{8a\pi^2 \cos^2\left(\frac{1}{2}a\cos(\varphi)\sin(\theta)\,n_{clad}k_0\right)}{(\pi^2 - a^2\cos^2(\varphi)\sin^2(\theta)n_{clad}^2k_0^2)^2}$$

$$|F_{sin}|^2 = \frac{32a\pi^2 \sin^2\left(\frac{1}{2}a\cos(\varphi)\sin(\theta)\,n_{clad}k_0\right)}{(4\pi^2 - a^2\cos^2(\varphi)\sin^2(\theta)n_{clad}^2k_0^2)^2}$$

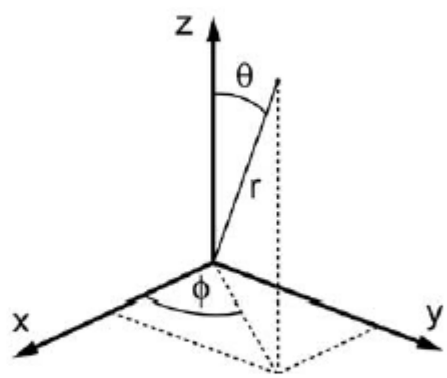

Figure 6 The coordinate system used in paper(reprint from [6])

Here n_{clad}, k_0, are constants waveguide transmission parameters we mentioned before. a is the height of the waveguide. φ, θ are the parameter that described the waveguide in the figure above. Using *Fcos* and *Fsin*, we evaluate far field pointing vector for TE and TM modes using:

$$\langle\vec{S}_{rough}^{TE}\rangle = \frac{|F_{cos}|^2\,\langle\left|F_{rough}\right|^2\rangle\left(\vec{S}_y + \gamma_{zy}\vec{S}_z\right)}{1+\gamma_{zy}}$$

$$\langle\vec{S}_{rough}^{TE}\rangle = \frac{\langle\left|F_{rough}\right|^2\rangle\left(|F_{cos}|^2\vec{S}_x + \gamma_{zx}|F_{sin}|^2\vec{S}_z\right)}{1+\gamma_{zx}}$$

Where $\gamma_{zy} = \frac{\int_{-\frac{a}{2}}^{\frac{a}{2}} |\vec{\Phi}(x',0)\cdot\hat{z}|^2 dx'}{\int_{-\frac{a}{2}}^{\frac{a}{2}} |\vec{\Phi}(x',0)\cdot\hat{y}|^2 dx'}$, $\gamma_{zx} = \frac{\int_{-\frac{a}{2}}^{\frac{a}{2}} |\vec{\Phi}(x',0)\cdot\hat{z}|^2 dx'}{\int_{-\frac{a}{2}}^{\frac{a}{2}} |\vec{\Phi}(x',0)\cdot\hat{x}|^2 dx'}$, $\Phi(d)$ is normalized so that

$$\int_{-\infty}^{\infty} \Phi^2(y)dy = 1$$

And the ensemble average of the roughness power array factor is

$$< |F_{rough}|^2 >= 2(2\mathrm{L})\tilde{R}(\beta + n_{clad}k_0 \sin{(\theta_c)} \sin{(\varphi_c)})$$

L is the length of waveguide, β is the propagation constant, k0 is the waveguide. All of these parameters we mentioned before. φ, θ are the angles to describe the waveguide in figure above. Here we need to use equation(16) to plug in to get the result we want.

At last using this *SrTE* and *SrTM*, calculating scattering loss per unit length by putting their values in relation given below:

$$\frac{P}{2L} = \oiint \left(\frac{\langle \vec{S}_{rough} \rangle}{2L} . \hat{r} \right) dA$$

Here we use *SrTE* and *SrTM* variable to hold this result and then a contour plot of *SrTE* and *SrTM* has been plot.

Result

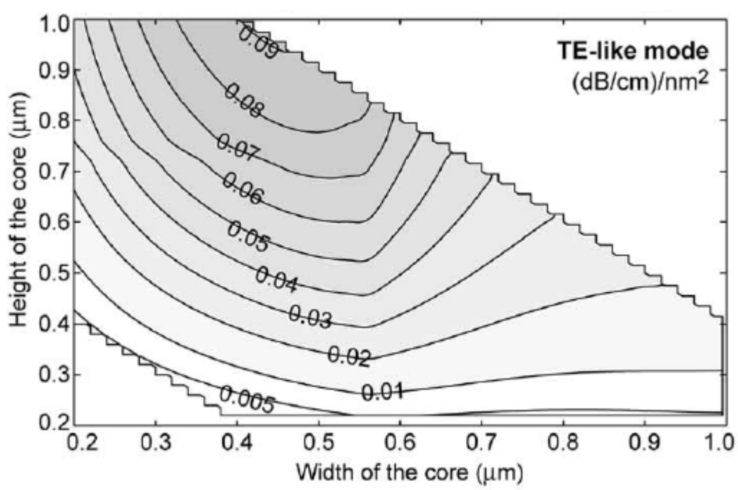

Figure 7(a) Scattering losses normalized to roughness variance(reprint from [6])

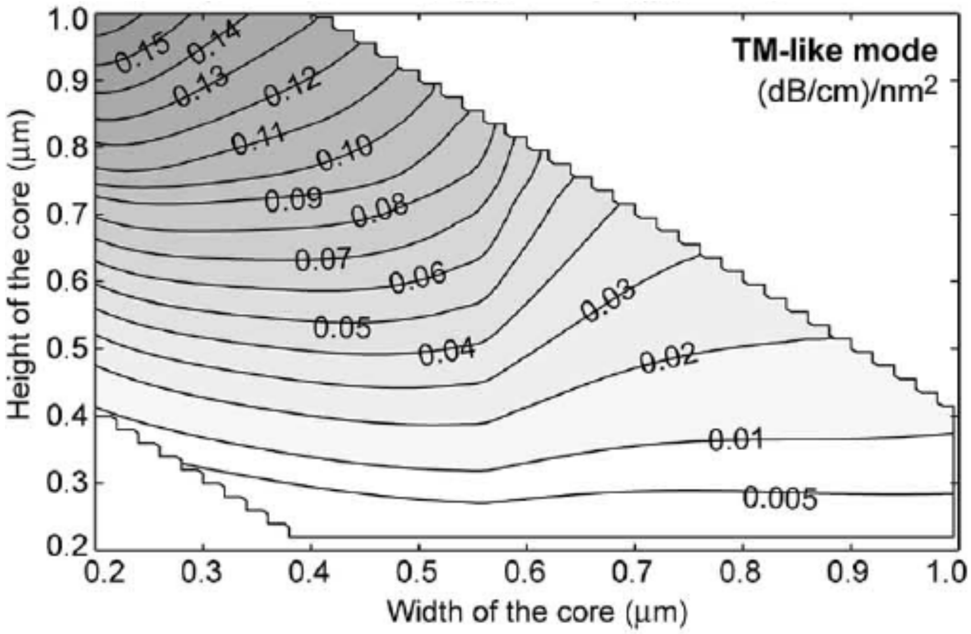

Figure 7(b) Scattering losses normalized to roughness variance(reprint from [6])

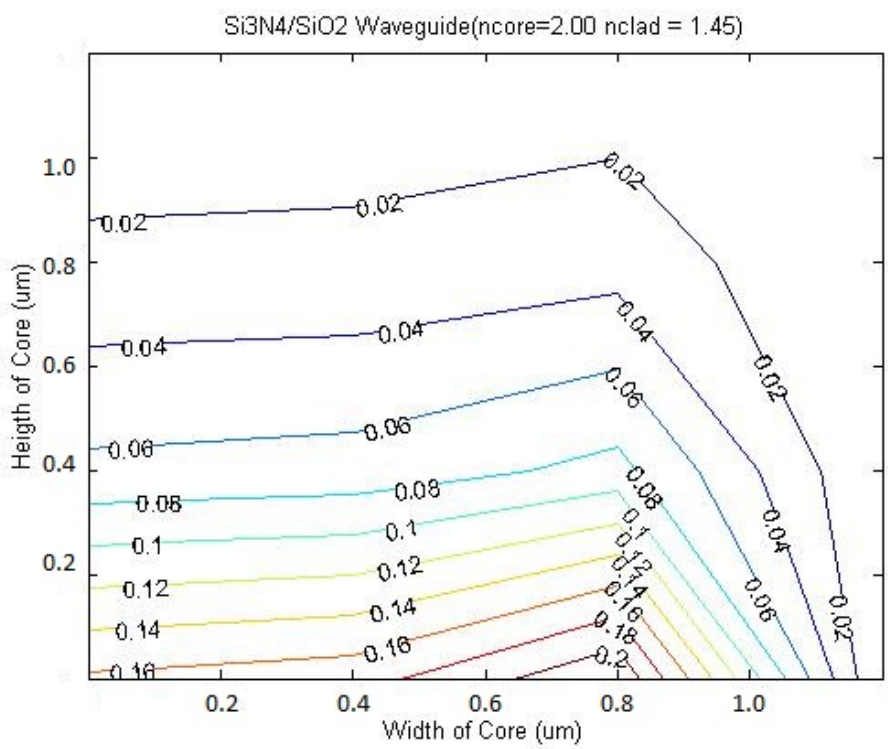

Figure 8 Scattering losses normalized to roughness variance(for TE mode)

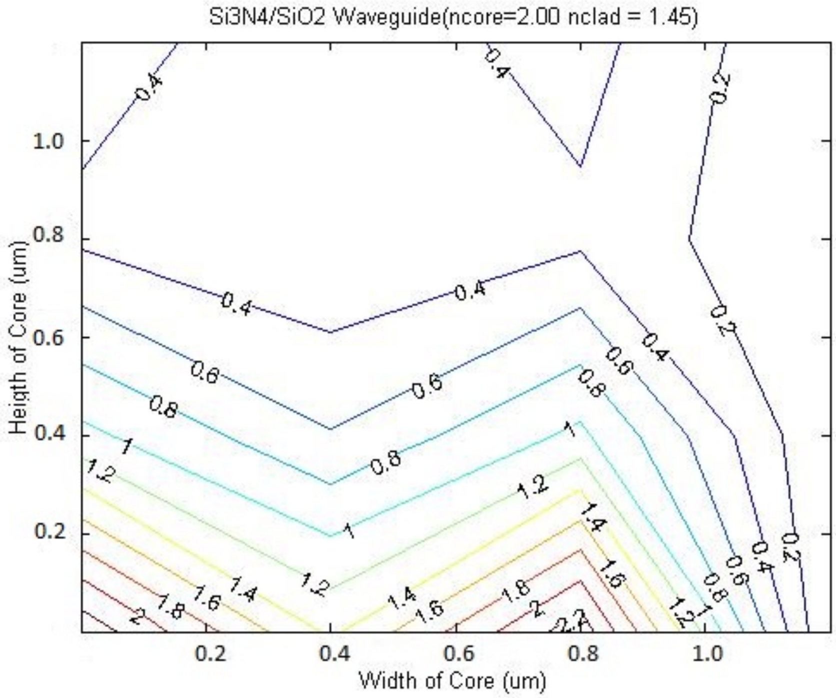

Figure 9 Scattering losses normalized to roughness variance(for TM mode)

From the result, we can see that Scattering losses show significant polarization dependence. Figures above are plotted for Si3N4/SiON waveguides, for which ncore=2.00 and nclad = 1.45. The figure 7(a) and figure 7(b) are got from paper[6]. Meanwhile I also tried to plot the figure myself, which display as figure8 and figure 9. However, the results are different from the paper. The difficulty here is to calculate the green function, which involves the knowledge of complicate mathematics integrations and also involve some quadrature calculation. Here I used matlab build-in library Quad to do the math. The other problem is the integrity involves some vector quadrature calculations. polarization dependence is dominated by the radiation efficiency, which is higher for the TM like mode. The TM-like mode is mainly x polarized while the TE-like mode is mainly y polarized[9].

Conclusion

Here we use two ways to do the analysis for both 2D and 3D. For 2D analyses, it is not as complicate as 3D. The 2D scattering losses theory bases on effective-index method. And it cannot predict how the waveguide cross section affects radiation efficiency. And also 2D analyses can misestimate scattering losses of small waveguides. For the 3D analysis, it is valid for any refractive-index contrast and field polarization which 2D analyses cannot. The way to do the 3D analyses is to start from low refractive-index-waveguide first and then extend to all index contrast. Through using 3D analysis we could improve the power losses estimate and to design a more efficient cross section of waveguide to minimize the scattering losses for roughness statistics.

4. Controlling temperature dependence of silicon waveguide

Nowadays, silicon-on-insulator(SOI) substrates are useful for many photonic integrated devices. But as we known, one of the fundamental issues to limit the performance is the high temperature sensitivity. For example, the arrayed waveguide grating(AWG) devices show the spectrum shift of about 80pm/K in the 1.55um wavelength region[21]. There are many solutions propose to minimize the influence of temperature sensitivity and two of them are popular solutions nowadays. One is to use a polymer overlay cladding which has negative TO coefficient. The other one is to use local heating to dynamically stabilize the devices. This can be finished by some different ways. Like external heater [14], direct heating through a bias current [15]or using the silicon itself to heat [16]. However, both of these two ways have their shortages. Polymer overlay cladding is not compatible with COMS and polymer cannot tolerate high temperature. And for the second ways, all of them require huge space and power consumption, which is not economic.

Here, the paper [17] create a way base on (M. Uenuma, 2009)[18]. The way they proposed to eliminate the temperature sensitivity is to change the thermo-optic effects of their interfering arms by their waveguide width and length optimization[18]. It is able to reduce the temperature sensitivity from 80pm/K to 28pm/K. And the paper [17] shows that they can make the thermal spectral shift close to near zero over a wide temperature range. The basic idea here is to make the thermo-optic effect between the two arms balance and maintain a certain phase difference between two arms [17]. Here is Figure 7 illustrates how the two arms waveguide works.

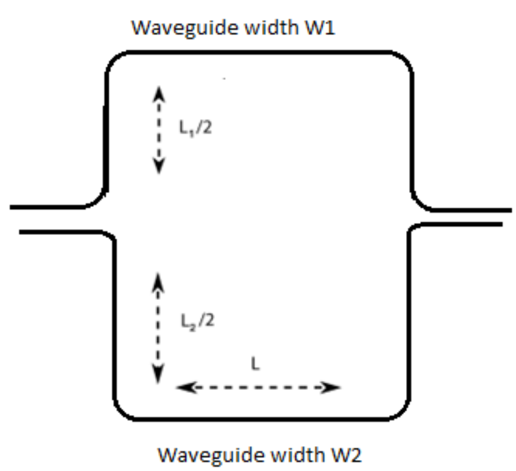

Figure 10 Schematic of the proposed device

The waveguide here consists of two arms and couples 3-dB directional couplers. One of the arms propagates at length of L horizontally and L_1 vertically. The other arm also propagates a length of L horizontally but instead of L_2 at vertical. For the width of the different arms, we can see from Figure7 that the up width W_1 is larger thanW_2.

As the paper[17] said, we can get the overall temperature dependence of the device as

$$m\lambda_0 = n_{eff}\Delta L + \Delta n_{eff} L$$

Where $\Delta L = L_2 - L_1$, $\Delta n_{eff} = n_{eff} W_2 - n_{eff} W_1$ and m here is the interference order at a given wavelengthλ_0. Here m can be an integer to give constructive interference at that wavelength or a half-integer to give destructive interference. Due to waveguide dispersion, the interference order is modified as

$$M = m - \frac{\Delta L \partial n_{eff}}{\partial \lambda} - \frac{L \partial (\Delta n_{eff})}{\partial \lambda}$$

M, n_{eff}, lambda and L are parameters we mentioned before. As a result, the temperature sensitivity of the wave spectrum is showed as

$$\frac{\Delta \lambda_0}{\Delta T} = \frac{\frac{\Delta L \partial n_{eff}}{\partial T} + \frac{L \partial (\Delta n_{eff})}{\partial T}}{M}$$

As we knew before, as the temperature changed, the spectrum of the wave would be shifted. Here $\Delta\lambda_0$ is the wavelength of the incident wave and the $\Delta\lambda_0$ represents the difference of wavelength between the shifted wave and the initial wave. So $\frac{\Delta\lambda_0}{\Delta T}$ represents the shift of wavelength per K changed and we can use that to display the temperature sensitive. Also, the above equation shows it can be shown that ΔL and Δe_{ff} are chosen appropriately with proper signs, the minima shift can be brought down to zero.

Base on the above theorem, the paper list some simulation result. First of all, we need to do the device fabrication to get the testing device. The device here combined a SOI wafer with 240 nm Si thickness and 3 mm buried oxide thickness. 100nm of silicon oxide was deposited on Si layer.

Also the oxide was etched by reactive ion etching(RIE). At last, the devices were cladded with 3mm of plasma enhanced chemical vapor deposition(PECVD) oxide.

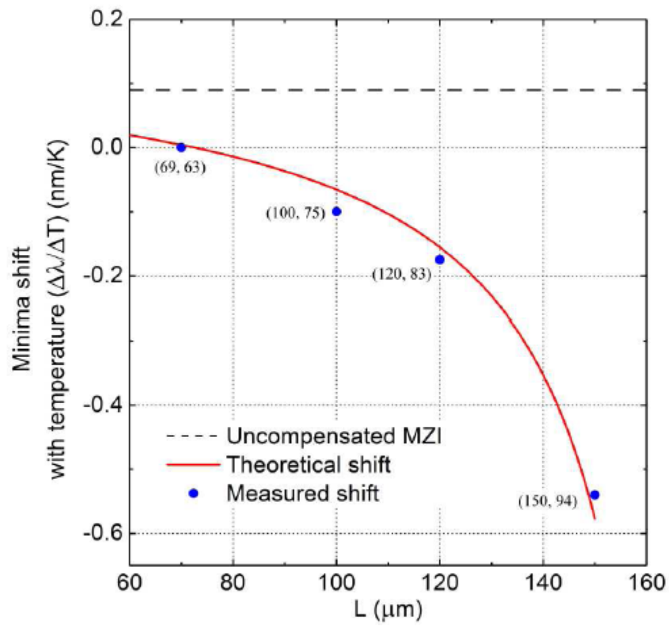

Figure 11 (reprint from [17]) Measured spectral shift with temperature compared with theoretically calculated values

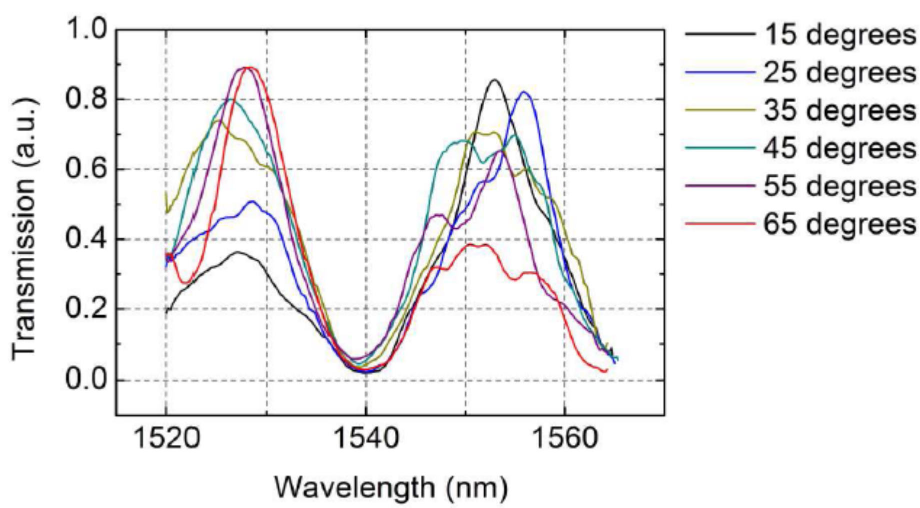

Figure 12(reprint from [17]) Operation of temperature insensitive MZI over 50 degrees

As the Figure 8 shows, the thermal spectral shifts agree well with the theoretically predicted values from the equation above. The data (69,63) means the temperature T is 69K and interference order m is 63 For this simulation, the W1 = 420nm and W2 = 190nm. The range of spectral shift could as large as -0.54 nm/K and as small as ~0.005 nm/K. From Figure 9 we can see that there is no significant shift in the transmission minima. For the experiment W1 = 420nm and W2 = 190nm, the interference order is 50.5 and initial wavelength is 1550 nm. The result shows that this temperature insensitive devices is fully scalable and applicable. And this proposed approach is applicable for any waveguide geometry – strip, slot and rib waveguides. Especially for rib waveguides, which would benefits a lot from the temperature insensitive device.

5.Propagation losses of silicon nitride waveguides(Si3N4)

Optical waveguides are one of the fundamental building blocks of microphotonics. The choice of the waveguide material determines the wavelength of the signal and the integration density. Stoichiometric silicon nitride Si_3N_4 for the core and silicon oxide SiO_2 for the cladding could be a suitable choice. Because of the large refractive index difference($\Delta n \approx 0.55$), the low scattering losses, the wide transparency window, and the compatibility with Si microelectronic technology.

The paper [22] shows that Si3N4/SiO2 multilayer(ML) waveguides can increase the optical confinement factor and reduce optical losses and did the experiment for both multilayer(ML) and singlelayer(SL) situation.

The way they people use to measure propagation losses was performed by using the insertion loss technique for various waveguide lengths. Waveguides have been measured by coupling-in light from laser diodes (1310 nm, 2 mW;1544 nm, 10 mW) or from a tunable laser s1500–1600 nm, 10 mW). The transmitted signal was imaged by a microscope objective. Data losses have been obtained by measuring five waveguides for each length typically five values from 0.5 to 5 cmd. The waveguide propagation loss coefficients of SL and ML waveguides are extracted by the slope of the insertion loss versus waveguide length curve. Here are the experiment results:

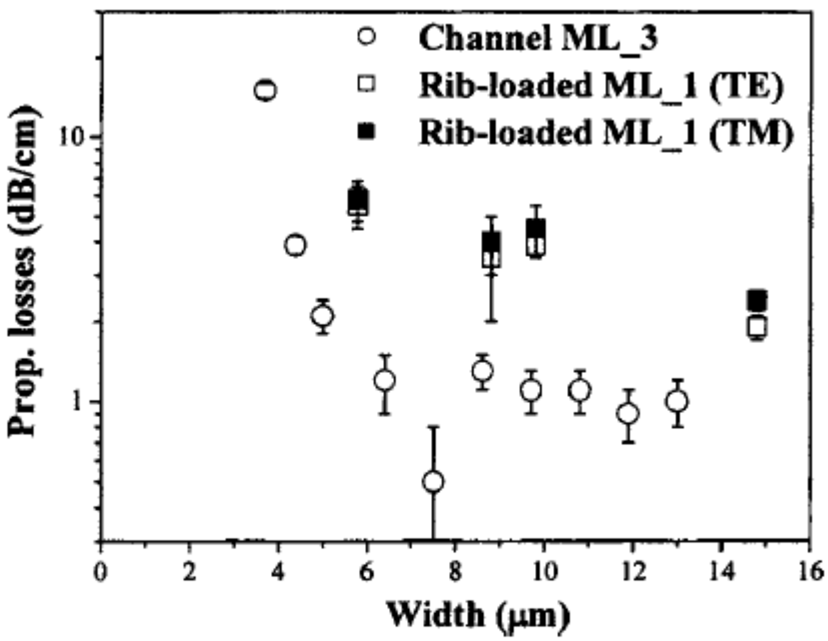

The figure above shows propagation losses at 1550 nm as a function of waveguide width in the two waveguide geometries. The increasing propagation losses with decreasing waveguide width are due to the increase of sidewalls scattering losses for rib-loaded waveguides

TABLE I. Propagation losses as a function of waveguide geometry for waveguide width larger than 10 μm. SL and ML refer to single layer and multilayer waveguides, respectively. The waveguide geometry and the silicon nitride etch depth, necessary for obtaining a rectangular structure, are also reported.

		Propagation losses (dB/cm)	
Samples	Waveguides	No polarized light	TE polarized light
SL_1	Channel (plasma etching, 200 nm etched)	4.5±0.5	···
SL_2	Strip loaded (plasma etching)	6.0±0.5	···
ML_1	Rib loaded (plasma etching, 40 nm etched)	···	1.9±0.2
ML_2	Rib loaded (plasma etching, 100 nm etched)	···	1.9±0.2
ML_3	Channel (plasma etching, 500 nm etched)	···	1.5±0.2

This table shows the waveguide propagation loss coefficients of SL and ML waveguide. The table also displays the propagation losses for different geometry of waveguides. The difference between channel (about 4.5 dB/cm) and strip-loaded (about 6 dB/cm) waveguides reflects analogous trends found at 780 nm.

Compare these result with Si/SiO2 we can found that the propagation losses is higher, but we can see Si_3N_4-based waveguides still have many advantages with respect to other systems:

1) In a wide wavelength range like from visible to the near infrared) the losses are much lower than others.
2) The layers Si3N4 used are compatible with CMOS processing.
3) The deposition process is easier compare with other material

References

[1] LadouceurLove, J.D., and Senden, T.J.F.,. (1994). Effect of side wall roughness in buried channel waveguides. IEE Proc., Optoelectron, 242-248.

[2]C.H. LeeJiangK. (2006.07). Sidewall roughness characterization and comparison between silicon and SU-8 microcomponents.

[3]Wim BogaertsBienstman, and Roel BaetsPeter. (2003). Scattering at sidewall roughness in photonic crystal slabs. Opt. Lett., 689-691.

[4]ChewC.W. (1995). Waves and Fields in Inhomogeneous Media. IEEE Press.

[5]F. GrillotVivien, E. Cassan and S. LavalL. (2008). Influence of waveguide geometry on scattering loss effects in submicron strip silicon-on-insulator waveguides. IET Optoelectron., 1-5.

[6]Barwiczand Haus, H.A.T.,. (2005). Three dimensional analysis of scattering losses due to sidewall roughness in microphotonic wavaguides. J. Light Technol, 891-896.

[7]ChatfieldC. (1989). The Analysis of Time Series—An Introduction (fourth ed.). Chapman and Hall, London.

[8]LayadiVonsovici, A., Orobtchouk, R., Pascal, D., and Koster, AA.,. (1998). Low-loss optical waveguide on standard SOI/SIMOX substrate. Opt. Commun., 31-33.

[9]MARK KUZNETSOVA. HAUSHERMANN. (1983). Radiation Loss in Dielectric Waveguide Structures by the Volume Current Method . IEEE J. Quantum Electron., 1505-1514.

[10]Payneand Lacey, J.P.R.:F.P.,. (1990). Radiation loss from planar waveguides with random wall imperfections. IEE Proc. Optoelectron., 282-288.

[11] F. GrillotVivien, S. Laval, D. Pascal and E. CassanL. (2004). Size influence on propagation loss induced by sidewall roughness in ultra small SOI waveguides. IEEE Photon. Tech. Lett. 16, 1661-1663.

[12] W. C. Chew and S. Y. Chen. (2003). Response of a point source embedded in a layered medium. IEEE Antennas Wireless Propag. Lett, 254 – 258.

[13] BarwiczTymon. (2005). 3D Analysis of scattering losses due to sidewall roughness in microphotonic waveguides: high index-contrast. Conference on Lasers & Electro-Optics.

[14] R. AmatyaW. Holzwarth, F. Gan, H. I. Smith, F. Kärtner, R. J. Ram, and M. A. PopovicC. (2007). Low Power Thermal Tuning of Second-Order Microring Resonators. Conference on Lasers and Electro-Optics/Quantum.

[15] S. ManipatruniK. Dokania, B. Schmidt, N. Sherwood-Droz, C. B. Poitras, A. B. Apsel, and M. LipsonR. (2008). Wide temperature range operation of micrometer-scale silicon electro-optic modulators. Opt. Lett, 2185 – 2187.

[16] M. R. WattsA. Zortman, D. C. Trotter, G. N. Nielson, D. L. Luck, and R. W. YoungW. (2009). Adiabatic Resonant Microrings (ARMs) with Directly Integrated Thermal Microphotonics. Conference on Lasers and Electro-Optics/International Quantum Electronics Conference.

[17]Biswajeet GuhaGondarenko and Michal LipsonAlexander. (2010). Minimizing temperature sensitivity of silicon Mach-Zehnder interferometers. OPTICS EXPRESS.

[18] M. UenumaT. Moookaand. (2009). Temperature-independent silicon waveguide optical filter. Opt. Lett. 34, 599-601.

[19]J. TengDumon, W. Bogaerts, H. Zhang, X. Jian, X. Han, M. Zhao, G. Morthier, and R. BaetsP. (2009). Athermal Silicon-on-insulator ring resonators by overlaying a polymer cladding on narrowed waveguides. Opt. Express, 14627 – 14633.

[20]M. HanA. Wang,and. (2007). Temperature compensation of optical microresonators using a surface layer with negative thermo-optic coefficient. Opt. Lett., 1800-1802.

[21]M. Uenuma, and T. Moooka, "Temperature-independent silicon waveguide optical filter," Opt. Lett. **34**(5), 599–601 (2009).

[22] M. Melchiorri,a! N. Daldosso, F. Sbrana, and L. Pavesi, G. Pucker, C. Kompocholis, P. Bellutti, and A. Lui, "Propagation losses of silicon nitride waveguides in the near-infrared range", Applied Physics Letter 86 (2005)

This work was partially supported by NSF award CCF-1218768.